A Muscle-Reflex Model that Encodes Principles of Legged Mechanics Produces Human Walking Dynamics and Muscle Activities

Hartmut Geyer, Hugh Herr, *Member, IEEE*

***Abstract*— While neuroscientists identify increasingly complex neural circuits that control animal and human gait, biomechanists find that locomotion requires little control if principles of legged mechanics are heeded that shape and exploit the dynamics of legged systems. Here we show that muscle reflexes could be vital to link these two observations. We develop a model of human locomotion that is controlled by muscle reflexes which encode principles of legged mechanics. Equipped with this reflex control, we find this model to stabilize into a walking gait from its dynamic interplay with the ground, reproduce human walking dynamics and leg kinematics, tolerate ground disturbances, and adapt to slopes without parameter interventions. In addition, we find this model to predict some individual muscle activation patterns known from walking experiments. The results suggest not only that the interplay between mechanics and motor control is essential to human locomotion, but also that human motor output could for some muscles be dominated by neural circuits that encode principles of legged mechanics.**

***Index Terms*— legged locomotion, feedback control, balance.**

I. Introduction

LEGGED locomotion of animals and humans is controlled by a complex network of neurons. Proposed in the early 20th century [1] and firmly established for animals today [2], the central pattern generator (CPG) forms the basis of this network. In the current view, the CPG consists of layers of neuron pools in the spinal cord [3] which, through other neuron pools channeling muscle synergies, provide rhythmic activity to the leg extensor and flexor muscles [4], [5] sufficient to generate stepping movements, even in the absence of spinal reflexes [6]. Spinal reflexes are nevertheless part of this complex network, contributing to the selection of locomotive patterns, the timing of the extensor and flexor activities, and the modulation of the CPG output [2], [7], [8]. Using this combination of a central pattern generation and modulating reflexes, neuromuscular models of lampreys [9], salamanders [10], cats [11]–[13], and humans [14], [15] have developed into essential tools for studying different control strategies in animal and human locomotion. The emphasis of these models has been to reproduce the architecture of the CPG and underlying reflexes suggested by experiments [7]. Little attention has however been paid to understanding how such architectures might represent or encode principles of legged mechanics.

Several principles of legged mechanics indicate that the seemingly complex task of locomotion control can largely be simplified. One such principle is mechanical self-stability. Using conceptual models of walking [16], [17] and running [18], [19] that capture the main features of legged mechanics, researchers have shown that legged locomotion self-stabilizes without control interventions if the mechanical components are properly tuned [20]–[23]. Walking and running robots have demonstrated the practical relevance and control benefits derived from mechanical self-stability [20], [24]–[26]. Another such principle is the reliance on compliant leg behavior. It has been shown that, if the legs behave similar to springs in stance, walking and running are only two out of many gaits of the same mechanical system which naturally emerge at different speeds without the need for a gait-specific control [27]. But it remains unclear if and how these and other principles of legged mechanics that simplify the control of locomotion are integrated into human motor control.

The natural candidates for such an integration are spinal reflexes, because they can link sensory information about legged mechanics directly into the activation of the leg muscles via alpha motoneurons, bypassing central inputs. For instance, in models of neuromuscular control, positive force feedback of leg extensor muscles has been shown to not only play an important role in load-bearing [28], but also generate compliant leg behavior in stance [29], suggesting that this key mechanical behavior can effectively be encoded in human motor control by a single muscle reflex. These conceptual models are however too simplistic to really compare predictions about motor control with the activity patterns observed for individual leg muscles.

To clarify the influence of legged mechanics on human motor control, we here develop a more detailed neuromuscular human model that expands on the idea of encoding principles of legged mechanics in autonomous muscle reflexes. The model represents the human body with a trunk and two three-segment legs. Each leg is actuated by seven Hill-type muscles

Manuscript received 20 February, 2009; revised 25 August, 2009, and 20 November, 2009; accepted 2 February 2010. The authors thank A. Prochazka and the anonymous reviewers for helpful comments and suggestions, which led to substantial improvements of the paper. This work was supported by an EU Marie-Curie Fellowship to HG (MOIF-CT-20052-022244).

H. Geyer is with the Robotics Institute, Carnegie Mellon University, 5000 Forbes Avenue, Pittsburgh, PA 15213, USA, e-mail: hgeyer@cs.cmu.edu.

H. Herr is with the Media Laboratory, Massachusetts Institute of Technology, Cambridge, MA 02139, USA, email: hherr@media.mit.edu.

that permit a direct comparison with prominent muscles of the human leg. In section 2, we detail how this model and its control evolve from the reliance on compliant leg behavior as a core principle of legged locomotion [18], [19], [27]. Throughout this process, we encode in muscle reflexes more principles of legged mechanics, for instance, to avoid joint overextension of segmented legs [30], [31], or to improve gait stability [23], [32]–[34]. Comparing the model's behavior with kinetic, kinematic, and electromyographic evidence from the literature, we show in section 3 that a neuromuscular model equipped with this principle-based motor control not only can produce biological walking mechanics, but also predicts the observed activation patterns of some individual muscles. We further show that this reflex control allows the model to tolerate ground disturbances and to adapt to slopes without parameter interventions. Finally, we discuss in section 4 the implications of our results.

II. Human Model

The conceptual basis for the human model is the bipedal spring-mass model (Fig. 1A), which simplifies human locomotion to a point mass that travels on two massless spring legs. Despite its simplicity, the bipedal spring-mass model reproduces the center-of-mass dynamics observed in human walking and running, unifying both gaits in one mechanical framework based on compliant leg behavior in stance [27]. To translate this conceptual model into a neuromuscular one, which better reflects human morphology, three main steps are required. First, the springs must be replaced with segmented legs, and compliant stance behavior must be generated by extensor muscles spanning the ankle and knee. Second, the point mass must be replaced with a trunk, and hip muscles must be added for its balance control. And third, swing leg control must be added to enable this model to enter cyclic locomotion.

In this section, we detail how the structure and control of the human model is guided by these three main steps. A major part of this model evolution is driven by principles of legged mechanics that we encode in muscle reflexes. Throughout this section, we try to motivate these reflexes with neurophysiological evidence from the literature.

A. Replacing the leg springs with segmented legs

In an earlier study, it was shown that positive force feedback (F+) of the extensor muscles, a spinal reflex during stance observed in cats [35] and suggested in humans [28], [36], can effectively generate compliant behavior in neuromuscular legs [29]. We thus replace each spring of the bipedal spring-mass model with a segmented leg that has thigh, shank and foot (Tab. IV), and add a soleus muscle (SOL) and a vasti muscle group (VAS) (Tab. II), both generating their own muscle activity in stance using F+ (Fig. 1B). We model this force reflex in the same way as in [29]. With F+, the stimulation $S_m(t)$ of a muscle m is the sum of a pre-stimulation $S_{0,m}$, and the muscle's time-delayed (Δt) and gained (G) force F_m: $S_m(t) = S_{0,m} + G_m F_m(t - \Delta t_m)$. Details on how reflex parameters were chosen are provided in the result section and appendix I. Appendix II describes how muscle stimulation translates into muscle force, and appendix III explains the model's musculoskeletal connections, joint architecture, and mass distribution.

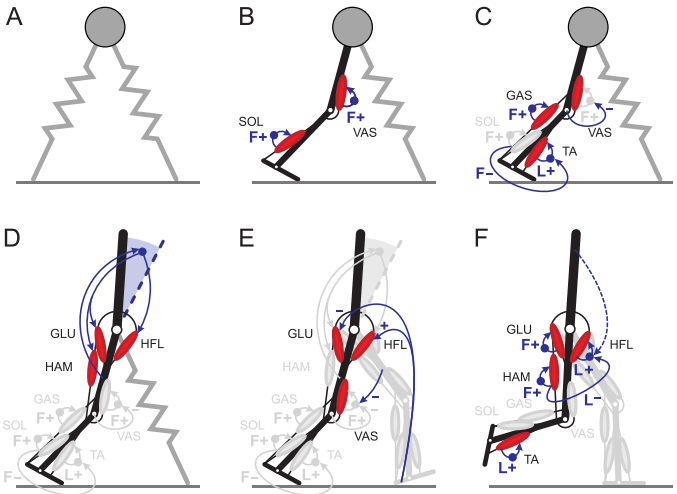

Fig. 1. Model evolution. *Stance leg*: (**A**) Compliant leg behavior as key to walk and run is generated (**B**) by driving the soleus muscle (SOL) and the lumped vasti group muscles (VAS) with positive force feedbacks F+. (**C**) To prevent knee overextension the biarticular gastrocnemius muscle (GAS) is added using F+, and the VAS gets inhibited if the knee extends beyond a 170° threshold. To prevent ankle overextension, the tibialis anterior muscle (TA) is added whose pulling of the ankle joint into a flexed position by positive length feedback L+ is suppressed under normal stance conditions by negative force feedback F- from soleus. *Trunk*: (**D**) The trunk is driven into a reference lean with respect to the vertical by the hip flexor (HFL) and co-activated hip extensor muscles (GLU, HAM) of the stance leg, where the biarticular HAM prevents knee overextension resulting from hip extensor moments. The trunk reflexes are modulated by the load the stance leg bears. *Swing leg*: (**E**) The landing of the other (leading) leg initiates swing by adding/subtracting a constant stimulation to HFL/GLU, respectively, and by suppressing VAS proportionally to the load borne by the other leg. (**F**) The actual leg swing is facilitated by HFL using L+ until it gets suppressed by L- of HAM. HFL's stimulation is biased dependent on the trunk's lean at take-off. Moreover, using F+ for GLU and HAM retracts and straightens the leg toward the end of swing. Finally, the now unsuppressed L+ of TA drives the ankle to a flexed position.

Although the segmentation into thigh, shank and foot is essential to represent the structure of the human leg, it also introduces a control problem during leg compression if the joints are compliant [30], [31], as guaranteed by F+ of SOL and VAS. In segmented legs, the knee and ankle torques, τ_k and τ_a, obey the static equilibrium $\tau_k/\tau_a = h_k/h_a$, where h_k and h_a are the perpendicular distances from the knee and the ankle to the vector of the leg ground reaction force (GRF), $\mathbf{F}_{leg}$, respectively. In effect, a large extension torque at one joint forces the other joint closer to $\mathbf{F}_{leg}$, threatening its overextension (for details see [30]).

We counter this tendency to overextend at the knee or the ankle by adding the gastrocnemius (GAS) and tibialis anterior (TA) muscles (Fig. 1C). Like SOL and VAS, the biarticular GAS uses F+ during the stance period of gait. This muscle reflex not only prevents knee hyperextension resulting from large extension torques at the ankle, but also contributes to generating an overall compliant leg behavior. In contrast, the monoarticular TA uses local positive length feedback (L+)

with $S_{TA}(t) = S_{0,TA} + G_{TA}(\ell_{CE,TA} - \ell_{off,TA})(t - \Delta_{t,TA})$ where $\ell_{CE,TA}$ is the TA fiber length and $\ell_{off,TA}$ is a length offset. Flexing the foot, TA's stretch reflex L+ prevents the ankle from overextending when large knee torques develop. However, this reflex is not required if sufficiently active ankle extensors preserve the torque equilibrium between the knee and ankle. To avoid that the TA unnecessarily fights the SOL in this situation, we inhibit the TA stimulation with a negative force feedback (F-) from the SOL, resulting in $S_{TA}(t) = S_{0,TA} + G_{TA}(\ell_{CE,TA} - \ell_{off,TA})(t - \Delta_{t,TA}) - G_{SOLTA}F_{SOL}(t - \Delta t_{SOL})$.

The implemented TA control is supported by evidence from reflex experiments. These experiments show that a large TA stretch response is present in swing, but suppressed mainly when TA is silent in stance [37], and it has been suggested that disynaptic Ia reciprocal pathways from ankle plantar flexors to dorsiflexors are responsible for this inhibition [38].

Without direct support from neurophysiological experiments, we further protect the knee from hyperextension by inhibiting VAS if the knee extends beyond a 170° threshold, $S_{VAS}(t) = S_{0,VAS} + G_{VAS}F_{VAS}(t - \Delta t_{VAS}) - k_\varphi \Delta\varphi_k(t - \Delta t_k)$, where k_φ is a proportional gain, $\Delta\varphi_k = \varphi_k - 170°$, and φ_k is the knee angle. This reflex inhibition is only active if $\Delta\varphi > 0$ and the knee is actually extending. In humans, it would require the sensory information from pressure cells around the knee joint capsule to translate into knee position and velocity.

B. Replacing the point mass with a trunk

For the next model evolution, we replace the point mass of the bipedal spring-mass model with a trunk segment (Tab. IV, Fig. 1D) that must be balanced during locomotion. Balancing the trunk is generally regarded as a multisensor integration task that mixes sensory information from the vestibular organs, visual cues, and proprioception from the leg muscles [39]. While this complex integration seems critical to control standing, it may not be required during locomotion [40]. In line with this observation, [41] could stabilize the trunk of a human model in walking only by activating the hip muscles proportional to the velocity of the trunk and to its forward lean in the inertial system.

We balance the trunk in a similar way. We add to each leg a gluteus muscle group (GLU) and a hip flexor muscle group (HFL). The GLU and the HFL are stimulated with a proportional-derivative signal of the trunk's forward lean angle θ with respect to gravity, $S_{GLU/HFL} \sim \pm[k_p(\theta - \theta_{ref}) + k_d\dot{\theta}]$, where k_p and k_d are the proportional and derivative gains, and θ_{ref} is a reference lean angle. This proportional-derivative trunk control can be interpreted as a reflex control that uses sensory information from the vestibular organs; however, it is not based on a particular principle of legged mechanics. In addition, we include the biarticular hamstring muscle group (HAM) with $S_{HAM} \sim S_{GLU}$ to counter knee hyperextension that results from a large hip torque developed by the GLU when pulling back the heavy trunk. Since hip torques can only balance the trunk if the legs bear sufficient weight on the ground, we modulate the stimulations of the GLU, HAM, and HFL for each leg proportionally to the amount of body weight it bears (shown as projection from the ipsilateral thigh in Fig. 1D). As a result, each leg's hip muscles contribute to the trunk's balance control only during stance.

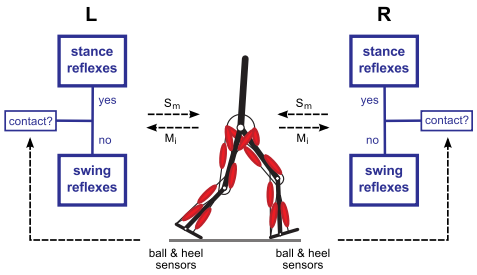

Fig. 2. Pattern generation. Instead of a central pattern, reflexes generate the muscle stimulations S_m. Left (L) and right (R) leg have separate stance and swing reflexes, which are selected based on contact sensing. The reflex outputs depend on mechanical inputs M_i intertwining mechanics and motor control.

C. Adding swing leg control

The human model's muscle-reflex control so far generates compliant leg behavior in stance while preventing joint overextension and balancing the trunk. To enable this model to enter cyclic locomotion, we add swing leg control.

We assume that the functional importance of each leg in stance reduces in proportion to the amount of body weight (bw) borne by the other leg, and thus initiate swing already in double support (Fig. 1E). The human model detects which leg enters stance last (contralateral leg), and inhibits F+ of the ipsilateral leg's VAS in proportion to the weight the contralateral leg bears, $S_{VAS}(t) = S_{0,VAS} + G_{VAS}F_{VAS}(t - \Delta t_{VAS}) - k_\varphi \Delta\varphi_k(t - \Delta t_k) - k_{bw}|\mathbf{F}_{leg}^{contra}|$ where k_{bw} is the weight gain and $\mathbf{F}_{leg}^{contra}$ the contralateral leg force. The contralateral inhibition allows the knee to break its functional spring behavior and flex while the ankle extends, pushing the leg off the ground and forward. Thus the ankle push-off commonly regarded as a major principle of gait to smooth the transition from the double support to the swing phase [16], [42] becomes an indirect outcome of the inhibition at the knee implemented to eliminate compliant leg behavior when it looses functional significance. In addition to the indirect push-off, the model further initiates swing by increasing the stimulation of the HFL, and decreasing that of the GLU, by a fixed amount ΔS in double support.

The implemented swing initiation reflects the current view on the peripheral control of the stance-to-swing transition. This view favors a mixed sensory input related to leg-unloading and hip positioning [43], where the first input is always required whereas the second one is more variable [44], and therefore, its actual implementation is less clear. It could moreover be shown that while unloading is essential, a direct input from the ipsilateral leg extensors via group-I afferents is not involved in the stance-to-swing transition [45]. By contrast, recent experiments on cockroach walking support a major role of the onset of another leg's stance in triggering the first leg's unloading [46].

During actual swing, we mainly rely on a leg's ballistic motion [16]. The distal leg muscles SOL, GAS, and VAS are silent in that phase. Only TA's L+, introduced in section II-A, remains active to provide foot clearance with the ground.

We modulate the ballistic motion in two necessary ways (Fig. 1F). First, as the natural frequency of the purely ballistic leg swing is too low to ensure a timely foot placement [16], the model's proximal HFL gets stimulated by its own stretch reflex L+, facilitating leg protraction during swing. Such a homonymous reflex-shaping of hip flexor activities has been suggested from experiments with decerebrate cats [47]; however, since the required protraction speed depends on the trunk's forward lean, in the human model HFL's L+ is biased by the trunk's pitch θ_{ref} at take off (TO), resulting in $S_{HFL}(t) = S_{0,HFL} + k_{lean}(\theta - \theta_{ref})_{TO} + G_{HFL}(\ell_{CE,HFL} - \ell_{off,HFL})(t - \Delta_{t,HFL})$.

Second, we improve gait stability by enforcing swing-leg retraction. If legs reach and maintain a proper orientation during swing, legged systems self-stabilize mechanically into a gait cycle [20]–[22], [27]. The tolerance of this mechanical self-stability against disturbances largely improves if a leg retracts before landing [23]. The human model realizes this halt-and-retract strategy with three muscle reflexes. One reflex inhibits the HFL's L+ proportional to the stretch which the HAM receives in swing, $S_{HFL}(t) = k_{lean}(\theta - \theta_{ref})_{TO} + G_{HFL}(\ell_{CE,HFL} - \ell_{off,HFL})(t - \Delta_{t,HFL}) - G_{HAMHFL}(\ell_{CE,HAM} - \ell_{off,HAM})(t - \Delta_{t,HAM})$. This negative length feedback L- compensates for the hip rotation that results from the transfer of angular momentum when the passive knee rotates into full extension during leg protraction. The other two reflexes, F+ of the GLU, $S_{GLU}(t) = S_{0,GLU} + G_{GLU}F_{GLU}(t - \Delta t_{GLU})$, and F+ of the HAM, $S_{HAM}(t) = S_{0,HAM} + G_{HAM}F_{HAM}(t - \Delta t_{HAM})$, ensure that, dependent on the actual protraction momentum, the swing leg not only halts, but also transfers part of this momentum into leg lowering and retraction.

Some neurophysiological evidence exists to support the implemented reflex control for leg retraction, though mainly for the hamstring. The excitation of the hamstring has been observed as a recovery strategy in late swing lowering the leg and shortening the step [48]. Moreover, this muscle group's tendon jerk reflex is enhanced in that phase, signaling a clear reflex contribution to its activation [49]. A similar reflex activity for the glutei has not been documented. Nor is a Ia reciprocal inhibition known that projects from the hamstring to the hip flexors in swing.

Although the human model has no central pattern generator (CPG) that feed-forwardly activates its muscles, it switches for each leg between the different reflexes for stance and swing using sensors at the ball and heel of each foot that detect ground (Fig. 2). These sensors mimic mechanoreceptors in the foot, which are suggested to be important for the control of phase transitions in humans [43].

III. Results

Because of the switches between stance and swing reflexes based on ground detection, the model's dynamic interaction with its mechanical environment becomes a vital part of generating muscle activities. To clarify the influence of legged mechanics on human motor control, we first try to make this model walk like a human and then compare its predicted motor output with muscle activations from the literature.

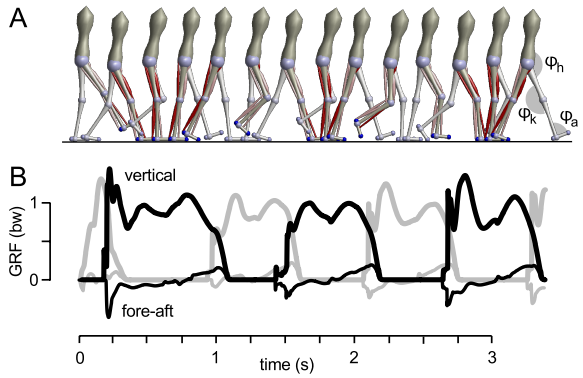

Fig. 3. Walking self-organized from dynamic interplay with ground. (**A**) Snapshots of human model taken every 250ms. Leg muscles shown only for the right leg with dark color for activations $> 10\%$. $\varphi_{a,k,h}$: ankle, knee and hip angle (initial conditions: $\varphi_{a,k,h} = 85°, 175°, 175°$ for left leg and $90°, 175°, 140°$ for right leg). (**B**) Corresponding model GRFs normalized to body weight (bw). Right and left leg GRFs shown in black and gray (30Hz low-pass filtered), with thick and thin traces marking the vertical and fore-aft components.

For the first part, we require the model (i) to produce cyclic motions with GRFs similar to those of human walking, (ii) to observe gait determinants relevant to sagittal-plane motion, including early stance knee flexion, controlled plantar flexion, powered plantar flexion and anterior-posterior flexion of the trunk [42], and (iii) to demonstrate some robustness against ground disturbances. We implement the model in Matlab SimMechanics (v2.7) and repeatedly start it from a typical walking speed of 1.3ms^{-1}, manually tuning the reflex parameters to match our mechanical requirements. As initial values for the reflex parameters, we use informed estimates. Note that all results are presented for the final values, which we obtain by maximizing (iii) constrained by (i) and (ii) (see appendix I for details on initial estimates and final values).

A. Walking gait

Figures 3 and 4 show the result of this manual reflex tuning. In figure 3, the model starts with its left leg in stance and its right leg in swing. Since the modeled muscle reflexes include signal transport delays of up to 20ms, all muscles are silent at first. Because of these disturbed initial conditions, the model slightly collapses and slows down in its first step (Fig. 3A). It recovers however in the next few steps, and walking self-organizes from the dynamic interplay between model and ground. Here the vertical GRF of the legs in stance shows the M-shape pattern characteristic for walking gaits (Fig. 3B), indicating similar center-of-mass dynamics of model and humans for steady-state walking. Here we consider the model to be in steady state only if its joint kinematics vary $<$ 1e-4 degrees from stride to stride.

B. Steady-state patterns of joint angles and torques

The reflex model produces angle and torque trajectories that are similar to those of human walking (Fig. 4). To quantify the agreement, we use the maximum cross-correlation coefficients R of model and human trajectories (human data digitized from [50] and then interpolated to 150 data points evenly distributed from 0% to 100% stride), and the corresponding time shifts Δ in percent of stride if significantly different from zero (95% confidence interval) [51]. R=1 shows a perfect agreement, whereas R=0 indicates no agreement. Because the model distinguishes between stance and swing control, we split the comparison into these two phases. The joint kinematics show a strong agreement for all joints in stance (φ_h: R=0.98, φ_k: R=0.97, φ_a: R=0.96), and for the hip and knee in swing (R=0.99). The ankle kinematics fit less well in that phase (R=0.63). The difference is due mainly to maximizing the model robustness against ground disturbances (compare Sec. III-D), which requires a rapid foot clearance not found in level walking. The joint torques nearly match for the ankle (τ_a: R=0.99), but show less agreement for the knee (τ_k: R=0.65) and lesser still for the hip (τ_h: R=0.45, Δ=10%). The major difference in the knee and hip torques occurs in early stance where, in the model, knee extension torque is diminished, and hip extension torque exaggerated and its onset delayed by about 5%. (Swing torques are not compared; [50] only reports stance torques.)

C. Predicted motor output

Figure 4 furthermore shows that the reflex model can not only produce human walking dynamics and kinematics, but also predicts known activation patterns. In stance, the correlations between predicted and measured activation patterns lie within the range observed in experiments [52] for all muscles. The patterns of SOL (R=0.97, Δ=9%) and GAS (R=0.99, Δ=9%) show the strongest agreement. The shift by 9% of stride in the predicted patterns is caused by the continued activity of the model's plantar flexors until the end of stance, and is related to the toe segment and associated muscles absent from the model. In humans, ankle plantar flexion in late stance is supported by toe flexors (and other small muscles crossing the subtalar joint) [50], which lessens the load on triceps surae. The patterns of GLU (R=0.93, Δ=6%) and HAM (R=0.90, Δ=7%) share similar features and have similar R-values and delays of onset in the model. The predicted VAS pattern (R=0.87, Δ=8%) captures the early stance activity in humans, but starts from a lower initial activity and shows a second peak not seen in experiments. The predicted TA pattern (R=0.87, Δ=3%) shares the lower initial activity, yet matches the remainder of TA's pattern in experiments. Finally, the muscle activity of HFL shows the weakest agreement (R=0.84) in stance.

In swing, the correlation reveals some experimental activation features unidentified by the model. The strongest agreement is observed for the HAM (R=0.95), although its overall activity is clearly too low in the model. The difference indicates that the HAM force is overestimated during swing in the model, which is supported by [53] who report that only

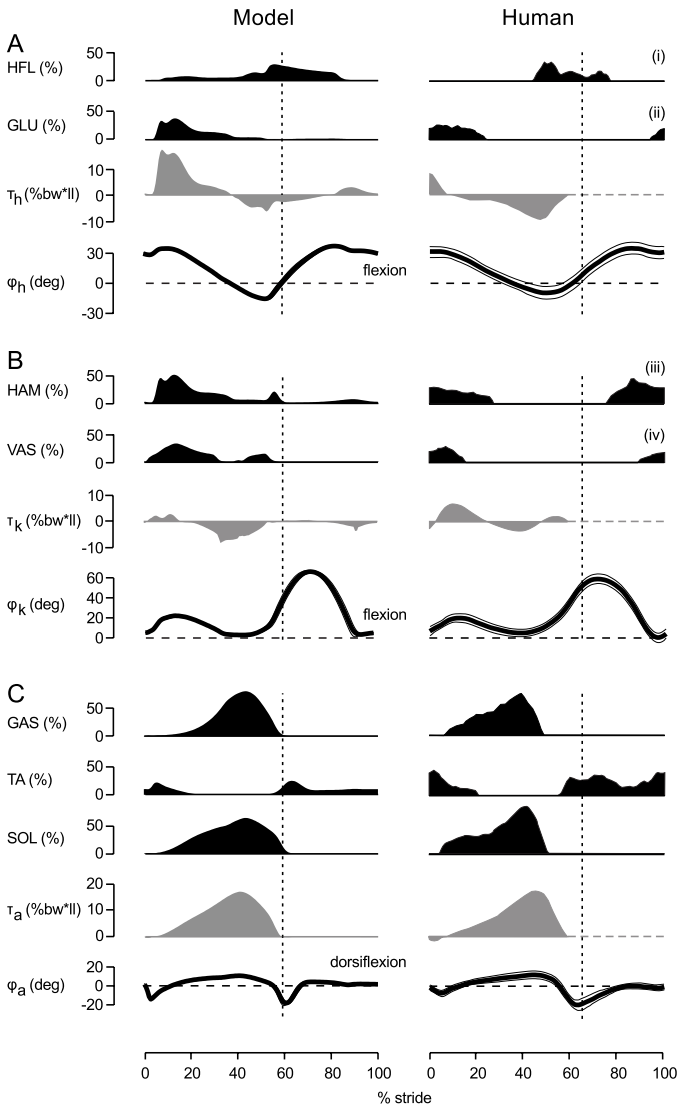

Fig. 4. Steady-state walking at 1.3ms^{-1}. Normalized to one stride from heel-strike to heel-strike of the same leg, the model's steady-state patterns of muscle activations, torques, and angles of (**A**) hip, (**B**) knee and (**C**) ankle are compared to human walking data (adapted from [50]). Vertical dotted lines around 60% of stride indicate toe off. Abbreviations are given in figure 1. Compared muscles: (i) adductor longus, (ii) upper gluteus maximum, (iii) semimembranosis, and (iv) vastus lateralis.

the semitendinosus muscle of the hamstrings influences swing leg motion. The patterns of HFL (R=0.87) and TA (R=0.87) show similar levels of agreement. One clear difference in the TA patterns occurs in late swing, where activity stays about constant in the model but rises in humans, preparing for stance [50]. The same feature is also lacking for GLU (R=0.51) and VAS (R=0.51) in the model, showing a clear mismatch in motor output.

The lack of stance preparation in the model explains the observable differences between model and human walking in stance. It causes the low initial stance activities of VAS and TA, which in turn results in an increased knee flexion (φ_k) and insufficient controlled plantar flexion (φ_a, τ_a). As a consequence, the model's trunk experiences a large forward tilt from the insufficiently damped impact when the forefoot

hits the ground, requiring the hip muscles GLU and HAM to generate exaggerated extension moments (τ_h) to maintain trunk balance (φ_h).

D. Adaptation to slopes

Despite its limited reflex control, the model shows robustness against small ground disturbances ($< \pm 4cm$) and can adapt to slopes ($< \pm 4\%$) without parameter interventions. Figure 5 provides an example in which the model encounters up (strides 2 to 6) and down slopes (strides 9 to 12) (see supplementary animation 1 for a trial in which the model encounters irregular terrain and longer slopes). No single control is responsible for this adaptation, but the dynamic interplay between legged mechanics and motor control. For instance, the compliance and rebound of the stance leg depends on how much load the leg extensors SOL, GAS and VAS experience, which guarantees that the leg yields sufficiently to allow forward progression when going up, but brakes substantially when going down (panels B and C). For another example, the motion of the swing leg is accelerated by the mechanical impact of the opposite leg, the forward lean of the trunk, and an increased ankle push-off. These combined features ensure that the swing leg protracts enough when going up and substantially so when going down (panel A), where the dynamic pull that GLU and HAM experience ensures that excess rotation of the leg is converted into rapid retraction and straightening (panel B).

Note however that for the maximum slopes of $\pm 4\%$ the model is sensitive to how the swing foot hits the ground. If the toe hits a step frontally when going up, or it touches the ground in mid-swing when going down, the model trips and can eventually fall. In general, we observe the model behavior to be very robust for the stance leg, but more sensitive to external disturbances and internal reflex adjustments for the swing leg (compare table I in appendix I for the sensitivity of the reflex parameters). For instance, if the model starts from an initial running speed of about 3ms^{-1}, it manages some steps that resemble human running, but eventually falls because the swing leg fails (see supplementary animation 2).

IV. Discussion

Our results suggest that mechanics and motor control cannot be viewed separately in human locomotion. We started from the assumption that principles of legged mechanics play an important role in locomotion and developed the conceptual spring-mass model, which explains the basic dynamics of human locomotion, into a neuromuscular one that resembles human morphology. For this development, we needed to encode several principles of legged mechanics with actuators and control, which turned into muscles and reflexes. Besides the generation of compliant stance-leg behavior [18], [19], [27], these principles included the stabilization of segmented chains against joint overextension when compressing in stance [30], [31], the indirect generation of ankle push-off [16], [42] by eliminating compliant leg behavior in proportion to its loss of functional significance in double support, the reliance mainly on ballistic motions for the lower leg in swing [16], and the improvement of gait stability by swing-leg retraction [23], [32]–[34]. While more principles of legged mechanics do certainly exist, the ones we implemented were sufficient for the human model to enter cyclic motions. Taken separately, these principles cannot account for human leg dynamics and kinematics at the level of detail we investigated; and there was no guarantee that taken together they would. However, we found after tuning the resulting muscle reflexes that, by combining these principles, human walking dynamics and leg kinematics emerge (Figs. 3 and 4), and the model tolerates ground disturbances and adapts to slopes without parameter interventions (Fig. 5). Moreover, we found that the model predicts some individual muscle activation patterns observed in walking experiments (Fig. 4). These results suggest that the interplay between mechanics and motor control is not only important, but could for some muscles dominate human motor output in locomotion.

Our findings support the view that centrally generated patterns of muscle activity may have limited functional relevance to normal locomotion. While it is generally accepted that CPGs can form a central drive for motor activity [4], [6], [54], their functional role in human locomotion is debated [43], [55]. On one side, it has been shown that locomotor-like activity of leg muscles can be evoked by tonic stimulation of the human spinal cord, favoring the existence and functional relevance of CPGs in man [5]. On the other side, the debate is fueled by the lack of direct experimental evidence of human CPGs, and by a continuing awareness that mechanics and motor control should be intertwined [7]. For instance, back in 1969, Lundberg [56] already suggested that, out of rather simple central patterns, spinal reflexes could shape the complex muscle activities seen in real locomotion. Refining this idea, Taga [57] later proposed that, because 'centrally generated rhythms are entrained by sensory signals which are induced by rhythmic movements of the motor apparatus ... [,] motor output is an emergent property of the dynamic interaction between the neural system, the musculo-skeletal system, and the environment'. In support of his claim, Taga [57] presented a neuromuscular model of human locomotion that combined a CPG with sensory feedback. He demonstrated how basic gait can emerge from the global entrainment between the rhythmic activities of the neural and musculo-skeletal systems.

What the actual ratio of central and reflex inputs is that generates the motor output remains unclear, however [12], [58], [59]. For instance, for walking cats, it has been estimated that only about 30 percent of the muscle activity observed in the weight bearing leg extensors can be attributed to muscle reflexes [60], [61]. In humans, the contribution of reflexes to the muscle activities in locomotion seems to be more prominent. Sinkjaer and colleagues estimated from unloading experiments that reflexes contribute about 50 percent to the soleus muscle activity during stance in walking [62]. More recently, Grey and colleagues found that the soleus activity changes proportionally to changes in the Achilles tendon force, suggesting a direct relationship between positive force feedback and activity for this muscle [36]. Whether such a large reflex contribution is present for all leg muscles is unclear. Perhaps the motor control of humans shows the same proximo-

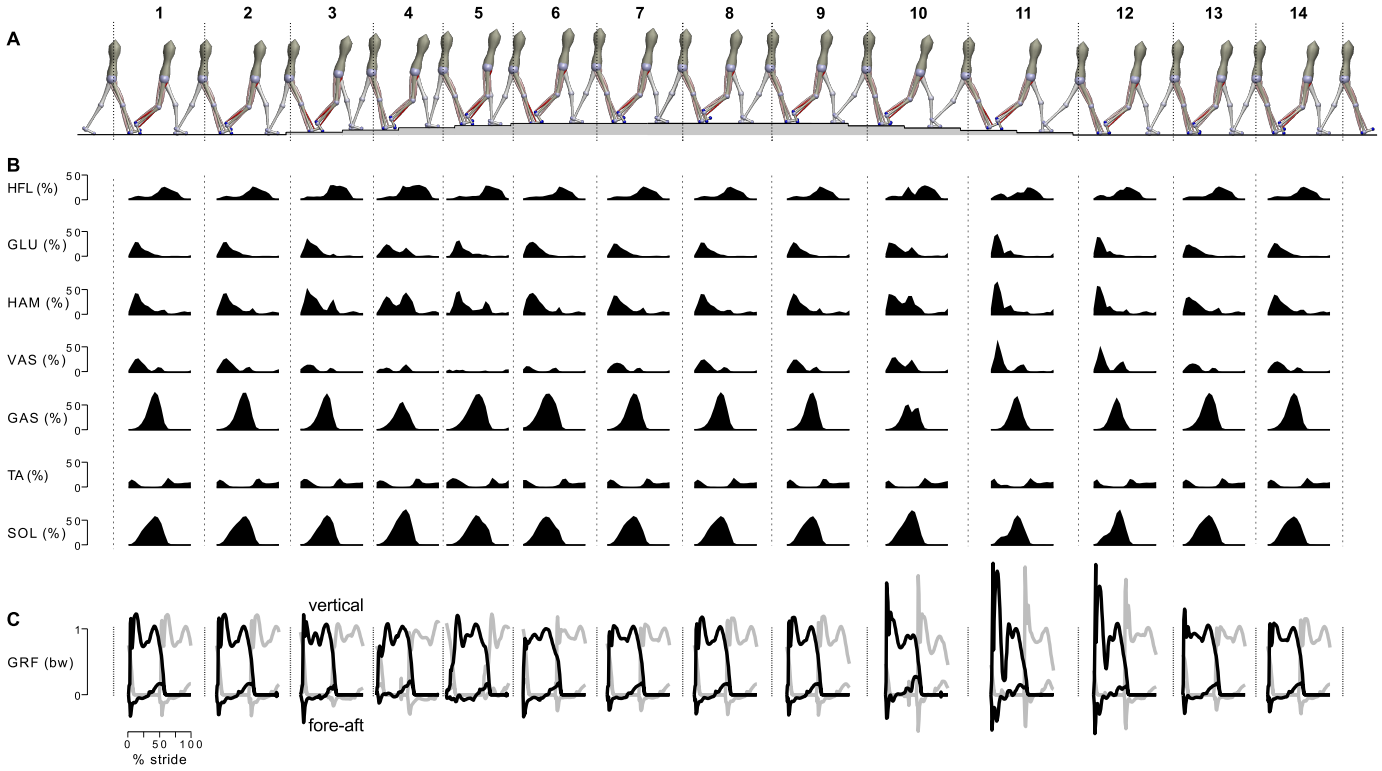

Fig. 5. Slope adaptation. Approaching from steady-state walking at 1.3ms^{-1}, 14 strides of the human model are shown adapting to slope ascent and descent with 4cm vertical steps. One stride is defined from heel-strike to heel-strike of the right leg. Shown are (**A**) snapshots of the model at heel-strike and toe-off of the right leg, (**B**) right leg muscle activation patterns, and (**C**) GRFs (right and left leg in black and gray) normalized to body weight (bw).

distal gradient as the one Daley and colleagues proposed for birds. They concluded from bird running experiments that proximal leg muscles are mainly controlled by central inputs while distal leg muscles are governed by reflex inputs due to higher proprioceptive feedback gains and a larger sensitivity to mechanical effects [63]. Having no CPGs, our model shows that no central input is required to generate walking motions and muscle activities, suggesting that reflex inputs which continuously mediate between the nervous system and its mechanical environment may even take precedence over central inputs in the control of normal human locomotion.

Experiments will be needed to probe this conclusion. Here, the principled approach detailed in this paper offers an advantage over the more common approach attempting to reverse-engineer human motor output. In many cases, neuromuscular models of animal and human locomotion mimic as many neural structures as suggested by physiological evidence, including CPGs, pattern formation and reflex networks [3], [11]–[15], [57]. Although these models can be optimized to generate locomotion steps, their predictive power is limited. The functional relevance of their individual control elements cannot be separated clearly. Nor can they reveal essential control structures that lie still undiscovered. The principled approach, by contrast, discards at first all the suggested control structures. Synthesizing motor control element by element, it allows to relate individual motor output to underlying mechanical function, and to make testable predictions about control elements that have not yet been described in experiments. Several muscle reflexes of the human model are currently not backed by physiological evidence (compare section II). They provide testable predictions about a motor control that encodes principles of legged mechanics.

While it is too early to draw definite conclusions about the neural consequences of our modeling results, the technical merit of the identified muscle-reflex control we demonstrate in a companion paper on the control of a powered ankle prosthesis.

APPENDIX I
REFLEX CONTROL PARAMETERS

Initial values for the reflex parameters were obtained from our previous study on reflex behavior, and from approximating the trunk as an inverted pendulum and the swing leg as a double pendulum driven at the hip. In detail, the F+ of SOL, GAS, and VAS (Sec. II-A, Fig. 1B,C) had initial reflex gains of $1/F_{max}$ and pre-stimulations of 1% reported to generate rebound behavior [29], and L+ of TA was adjusted to dorsiflex the ankle to $5\,\mathrm{deg}$ in 100ms. For the trunk balance (Sec. II-B, Fig. 1D), the gains k_p and k_d, and the pre-stimulation S_0, were initially set to balance and critically damp the inverted trunk pendulum with a natural frequency of 2Hz and a forward lean of $5\,\mathrm{deg}$ (typical values in human walking), assuming actuators with a maximum force of 3000N and a lever of 10cm. The gain k_{bw} was then adjusted so that one body weight fully suppressed muscle activation. For the swing leg control (Sec. II-C, Fig. 1E,F), ΔS of HFL and GLU had a start value sufficient to generate a step from stand still of the model. The L+ reflex gain of HFL was adjusted so that a double pendulum

TABLE I

REFLEX PARAMETERS AND THEIR TOLERANCE. THE GAINS G_m AND k_{bw} ARE NORMALIZED TO $F_{max,m}$ AND THE BODY WEIGHT. THE OFFSETS $\ell_{off,m}$ ARE SHOWN IN FRACTIONS OF $\ell_{opt,m}$. PRE-STIMULATIONS $S_{0,m}$ ARE 0.01 (NOT SHOWN) EXCEPT FOR THE STANCE VALUES $S_{0,VAS}$ AND $S_{0,BAL}$ OF THE VAS AND OF THE TRUNK BALANCE MUSCLES HAM, GLU AND HFL.

	value	min ... max		value	min ... max
G_{SOL}	1.2	0.97 ... 2.17	θ_{ref}	0.105	0.017 ... 0.11
G_{TA}	1.1	0.55 ... 3.2	k_d	0.25	0.10 ... 0.75
$\ell_{off,TA}$	0.71	0.59 ... 0.80	k_{bw}	1.2	1.3 ... 5.0
G_{SOLTA}	0.3	0 ... ∞	ΔS	0.25	0.14 ... 1
G_{GAS}	1.1	0 ... ∞	G_{HAM}	0.65	0 ... 0.67
$S_{0,VAS}$	0.09	0.047 ... 0.71	G_{GLU}	0.4	0 ... 0.52
G_{VAS}	1.15	0.82 ... 13.5	G_{HFL}	0.35	0.17 ... 3
k_φ	2	0 ... ∞	$\ell_{off,HFL}$	0.6	0 ... 0.67
$\varphi_{k,off}$	2.97	2.71 ... ∞	G_{HAMHFL}	4	0 ... 100
$S_{0,BAL}$	0.05	0.01 ... 0.32	$\ell_{off,HAM}$	0.85	0.83 ... ∞
k_p	1.91	1.78 ... 22	k_{lean}	1.15	1 ... 5.7

of a lifted thigh and a passive shank-foot reaches a step length of 0.7m within 300ms (typical values for normal walking). Since the ankle push-off from a stand still does not suffice, the driven pendulum physics require that the thigh decelerates eventually allowing the inertia of the shank-foot to passively rotate it around the thigh and bring the leg into extension, which guided setting the reflex gain and offset of the L- from HAM to HFL. The reflex gains of the F+ of GLU and HAM were initially set to $0.5/F_{max}$, which resulted in a gentle leg lowering and retraction of the double pendulum toward the end of the step with 0.7m length. Finally, the manual reflex tuning that followed also delivered the necessary values for the remaining reflexes including the suppressions of TA via F- from SOL and of VAS via knee angle feedback (Sec. II-A), and the trunk bias of HFL's L+ in swing (Sec. II-C). The final value for each reflex parameter is shown in table I along with its sensitivity (a change during steady-state locomotion beyond the min/max limits leads to a fall).

The equations below implement the reflex control computing the muscle stimulations $S_m(t)$. All stimulations are limited from 0.01 to 1 before they produce muscle activations $A_m(t)$. The time delays of 20ms, 10ms and 5ms in the equations represent long, medium and short neural signal delays. They were not tuned but estimated from the time gaps between M-wave and H-wave of H-reflex experiments (for details see [29]).

Stance Reflexes ($t_l = t - 20ms$, $t_m = t - 10ms$, and $t_s = t - 5ms$, DSup is 1 if leg is trailing leg in double support, otherwise 0, $\{\}_{+/-}$ refers to only positive/negative values): $S_{SOL} = S_{0,SOL} + G_{SOL}\ F_{SOL}(t_l)$; $S_{TA} = S_{0,TA} + G_{TA}\left[\ell_{ce,TA}(t_l) - \ell_{off,TA}\right] - G_{SOLTA} F_{SOL}(t_l)$; $S_{GAS} = S_{0,GAS} + G_{GAS} F_{GAS}(t_l)$; $S_{VAS} = S_{0,VAS} + G_{VAS}\ F_{VAS}(t_m) - k_\varphi\left[\varphi_k(t_m) - \varphi_{k,off}\right]\left[\varphi_k(t_m) > \varphi_{k,off}\right]\left[\dot{\varphi}_k(t_m) > 0\right] - k_{bw}\ \left|\mathbf{F}^{contra}_{leg}(t_s)\right|\ DSup$; $S_{HAM} = S_{0,HAM} + \left\{k_p\left[\theta(t_s) - \theta_{ref}\right] + k_d\dot{\theta}(t_s)\right\}_+ k_{bw}\left|\mathbf{F}^{ipsi}_{leg}(t_s)\right|$; $S_{GLU} = S_{0,GLU} + \left\{0.68 k_p\left[\theta(t_s) - \theta_{ref}\right] + k_d\dot{\theta}(t_s)\right\}_+ k_{bw}\ \left|\mathbf{F}^{ipsi}_{leg}(t_s)\right| - \Delta S\ DSup$; $S_{HFL} = S_{0,HFL} + \left\{k_p\left[\theta(t_s) - \theta_{ref}\right] + k_d\dot{\theta}(t_s)\right\}_- k_{bw}\left|\mathbf{F}^{ipsi}_{leg}(t_s)\right| + \Delta S\ DSup$

Swing reflexes ($\{\}_{PTO}$: constant value taken at previous take off): $S_{SOL} = S_{0,SOL}$; $S_{TA} = S_{0,TA} + G_{TA}\left[\ell_{ce,TA}(t_l) - \ell_{off,TA}\right]$; $S_{GAS} = S_{0,GAS}$; $S_{VAS} = S_{0,VAS}$; $S_{HAM} = S_{0,HAM} + G_{HAM}\ F_{HAM}(t_s)$; $S_{GLU} = S_{0,GLU} + G_{GLU}\ F_{GLU}(t_s)$; $S_{HFL} = S_{0,HFL} + G_{HFL}\left[\ell_{CE,HFL}(t_s) - \ell_{off,HFL}\right] - G_{HAMHFL}\left[\ell_{CE,HAM}(t_s) - \ell_{off,HAM}\right] + \left\{k_{lean}\left[\theta(t_s) - \theta_{ref}\right]\right\}_{PTO}$

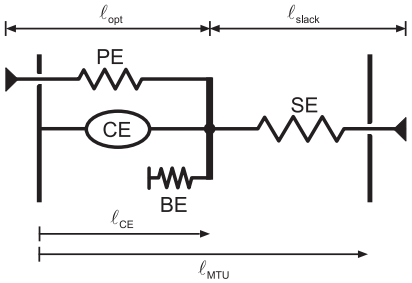

Fig. 6. Muscle-tendon model. An active, contractile element (CE) together with a series elasticity (SE) form the muscle-tendon unit (MTU) in normal operation. If the CE stretches beyond its optimum length ($\ell_{CE} > \ell_{opt}$), a parallel elasticity (PE) engages. Conversely, a buffer elasticity (BE) prevents the active CE from collapsing if the SE is slack ($\ell_{MTU} - \ell_{CE} < \ell_{slack}$).

APPENDIX II
MUSCLE TENDON UNITS

All 14 muscle-tendon units (MTUs) have a common model structure (Fig. 6). An MTU's force $F_m = F_{se} = F_{ce} + F_{pe} - F_{be}$ is computed from resolving the inner degree of freedom ℓ_{ce}. With $F_{ce} = AF_{max} f_\ell(\ell_{ce}) f_v(v_{ce})$, ℓ_{ce} is equal to $\int v_{ce} dt = \int [f_v(v_{ce})]^{-1} dt$ with $f_v(v_{ce}) = \frac{F_{se} - F_{pe} + F_{be}}{AF_{max} f_\ell(\ell_{ce})}$, where A is the muscle activation, F_{max}, the maximum isometric force, $f_\ell(\ell_{ce})$ and $f_v(v_{ce})$ are the force-length and force-velocity relationships of the contractile element (CE), and F_{se}, F_{pe} and F_{be} are the forces of the series (SE), parallel (PE), and buffer elasticity (BE). Details on how we model A, f_ℓ, f_v and F_{se} are given in [29]; for completeness, we here report the parameters required to compute these functions including the excitation-contraction coupling constant $t_{ecc} = 0.01$ of A; the width $w = 0.56\ell_{opt}$ and the residual force factor $c = 0.05$ of f_ℓ; the eccentric force enhancement $N = 1.5$ and the shape factor $K = 5$ of f_v; and the reference strain $\varepsilon_{ref} = 0.04$ of F_{se}. $F_{be} = F_{max}(\frac{\ell_{min} - \ell_{ce}}{\ell_{opt}\varepsilon_{be}})^2$, where $\ell_{min} = \ell_{opt} - w$ is the BE rest length and $\varepsilon_{be} = w/2$ is a reference compression. $F_{pe} = F_{max}(\frac{\ell_{ce} - \ell_{opt}}{\ell_{opt}\varepsilon_{pe}})^2\ f_v(v_{ce})$ with the PE reference strain $\varepsilon_{pe} = w$. $F_{pe} \sim f_v(v_{ce})$ allows to rewrite $f_v(v_{ce}) = \frac{F_{se} + F_{be}}{AF_{max} f_\ell(\ell_{ce}) + F^*_{pe}}$ with $F^*_{pe} = F_{max}(\frac{\ell_{ce} - \ell_{opt}}{\ell_{opt}\varepsilon_{pe}})^2$, which can robustly be integrated with coarse time steps, because it cannot run into negative results $f_v(v_{ce}) < 0$. Note that PE and BE engage outside the normal range of operation of the MTU and play minor roles for its dynamics in locomotion. The MTUs share the same parameters except for four main ones that distinguish individual muscle physiology (Tab. II).

APPENDIX III
MTU ATTACHMENTS AND SEGMENT PROPERTIES

The MTUs connect to the skeleton by spanning one or two joints (Tab. III). The transfer from MTU force F_m to joint

TABLE II

INDIVIDUAL MTU PARAMETERS. VALUES ARE ESTIMATED FROM [64] ASSUMING A FORCE OF 25N PER CM^2 CROSS SECTIONAL AREA (F_{max}), MAXIMUM SPEEDS OF $6\ell_{opt}s^{-1}$ AND $12\ell_{opt}s^{-1}$ FOR SLOW AND MEDIUM-FAST TWITCH MUSCLES (v_{max}), AND ℓ_{opt} AND ℓ_{slack} TO REFLECT MUSCLE FIBER AND TENDON LENGTHS.

	SOL	TA	GAS	VAS	HAM	GLU	HFL
$F_{max}(N)$	4000	800	1500	6000	3000	1500	2000
$v_{max}(\ell_{opt}s^{-1})$	6	12	12	12	12	12	12
$\ell_{opt}(cm)$	4	6	5	8	10	11	11
$\ell_{slack}(cm)$	26	24	40	23	31	13	10

TABLE III

MTU ATTACHMENT PARAMETERS (VALUES MOTIVATED FROM [65]–[68] OR ANATOMICAL ESTIMATES).

	ankle			**knee**			**hip**		
	SOL	TA	GAS	GAS	VAS	HAM	HAM	GLU	HFL
$r_0(cm)$	5	4	5	5	6	5	8	10	10
$\varphi_{max}(deg)$	110	80	110	140	165	180	-	-	-
$\varphi_{ref}(deg)$	80	110	80	165	125	180	155	150	180
ρ	0.5	0.7	0.7	0.7	0.7	0.7	0.7	0.5	0.5

torque τ_m is modeled as $\tau_m = r_m(\varphi)F_m$, where the lever $r_m(\varphi)$ equals r_0 for the hip and $r_0\cos(\varphi - \varphi_{max})$ for the ankle and knee. Here φ is the joint angle and r_m gets maximal at φ_{max}. Changes in MTU length are modeled as $\Delta\ell_{mtu} = \rho r(\varphi - \varphi_{ref})$ for the hip and as $\Delta\ell_{mtu} = \rho r[\sin(\varphi - \varphi_{max}) - \sin(\varphi_{ref} - \varphi_{max})]$ for the ankle and knee, where φ_{ref} is the joint angle at which $\ell_{mtu} = \ell_{opt} + \ell_{slack}$, and ρ accounts for muscle pennation angles and ensures that the MTU fiber length stays within physiological limits throughout the joint work space.

The model's segments are rigid bodies specified by their mass m_S, inertia Θ_S, and length ℓ_S, and the positions $d_{G,S}$ of the local center of mass and $d_{J,S}$ of the proximal joint measured from the distal end (Tab. IV). The segments are connected by revolute joints with ranges of operation, $70° < \varphi_a < 130°$, $\varphi_k < 175°$ and $\varphi_h < 230°$, outside of which soft limits engage (see appendix IV).

APPENDIX IV
GROUND CONTACTS AND JOINT LIMITS

The model's foot segments have toe and heel contact points (CPs). A CP's vertical GRF is modeled as $F_y = k_y\Delta y_{cp}(1 + \Delta\dot{y}^*_{cp})(\Delta y_{cp} > 0)(\Delta\dot{y}^*_{cp} > -1)$, where $k_y = 81.5kN/m$ is the vertical contact stiffness, Δy_{cp}, ground penetration, and $\Delta\dot{y}^*_{cp}$, its velocity normalized to $v_{max} = 3cms^{-1}$. This nonlinear spring-damper model is motivated from the literature [41], [69], but interprets contacts with two basic material properties:

TABLE IV

SEGMENT PARAMETERS (VALUES APPROXIMATED FROM [41]).

	Feet	Shanks	Thighs	Trunk
$\ell_S(cm)$	20	50	50	80
$d_{G,S}(cm)$	14	30	30	35
$d_{J,S}(cm)$	16	50	50	-
$m_S(kg)$	1.25	3.5	8.5	53.5
$\Theta_S(kgm^2)$	0.005	0.05	0.15	3

ground stiffness k_y and maximum relaxation speed v_{max}. Here $v_{max} = \infty$ or 0 describes a perfectly elastic or inelastic impact. Note that we use the same model for the joint soft limits with $k_j = 0.3Nm\deg^{-1}$ and $v_{max,j} = 1\deg s^{-1}$. A CP's horizontal GRF is modeled as either sliding force $F_{x,sl} = -sgn(\dot{x}_{cp})\mu_{sl}F_y$ or stiction force $F_{x,st} = -k_x\Delta x_{cp}(1 + sgn(\Delta x_{cp})\Delta\dot{x}^*_{cp})$, where $\dot{x}_{cp}$ is the CP's horizontal velocity, $\mu_{sl} = 0.8$, the sliding friction coefficient, $k_x = 8.2kN/m$, the horizontal contact stiffness, $\Delta x_{cp} = x_{cp} - x_0$, the shift from the point x_0 at which stiction engaged, and $\Delta\dot{x}^*_{cp}$, its velocity again normalized to v_{max}. A CP engages in stiction if $|\dot{x}_{cp}| < 1cms^{-1}$ and returns to sliding if $F_{x,st} \geq \mu_{st}F_y$ with a stiction coefficient $\mu_{st} = 0.9$.

REFERENCES

[1] T. G. Brown, "On the nature of the fundamental activity of the nervous centres; together with an analysis of the conditioning of rhythmic activity in progression, and a theory of the evolution of function in the nervous system." *J Physiol*, vol. 48, no. 1, pp. 18–46, 1914.

[2] G. Orlovsky, T. Deliagina, and S. Grillner, *Neuronal control of locomotion: from mollusc to man*. Oxford University Press, New York, 1999.

[3] I. A. Rybak, N. A. Shevtsova, M. Lafreniere-Roula, and D. A. McCrea, "Modelling spinal circuitry involved in locomotor pattern generation: insights from deletions during fictive locomotion." *J Physiol*, vol. 577, no. Pt 2, pp. 617–639, 2006.

[4] V. Dietz, "Spinal cord pattern generators for locomotion." *Clin Neurophysiol*, vol. 114, no. 8, pp. 1379–1389, 2003.

[5] K. Minassian, I. Persy, F. Rattay, M. M. Pinter, H. Kern, and M. R. Dimitrijevic, "Human lumbar cord circuitries can be activated by extrinsic tonic input to generate locomotor-like activity." *Hum Mov Sci*, vol. 26, no. 2, pp. 275–295, 2007.

[6] S. Grillner and P. Zangger, "On the central generation of locomotion in the low spinal cat." *Exp Brain Res*, vol. 34, no. 2, pp. 241–261, 1979.

[7] K. Pearson, O. Ekeberg, and A. Buschges, "Assessing sensory function in locomotor systems using neuro-mechanical simulations." *Trends Neurosci*, vol. 29, no. 11, pp. 625–631, 2006.

[8] B. W. Verdaasdonk, H. F. J. M. Koopman, and F. C. T. Van der Helm, "Resonance tuning in a neuro-musculo-skeletal model of the forearm," *Biol Cybern*, vol. 96, no. 2, pp. 165–80, 2007.

[9] O. Ekeberg and S. Grillner, "Simulations of neuromuscular control in lamprey swimming." *Philos Trans R Soc Lond B Biol Sci*, vol. 354, no. 1385, pp. 895–902, 1999.

[10] A. Ijspeert, A. Crespi, D. Ryczko, and J.-M. Cabelguen, "From swimming to walking with a salamander robot driven by a spinal cord model," *Science*, vol. 315, no. 5817, pp. 1416–1420, 2007.

[11] D. G. Ivashko, B. I. Prilutski, S. N. Markin, J. K. Chapin, and I. A. Rybak, "Modeling the spinal cord neural circuitry controlling cat hindlimb movement during locomotion," *Neurocomputing*, vol. 52–54, pp. 621–629, 2003.

[12] A. Prochazka and S. Yakovenko, "The neuromechanical tuning hypothesis." *Prog Brain Res*, vol. 165, pp. 255–265, 2007.

[13] C. Maufroy, H. Kimura, and K. Takase, "Towards a general neural controller for quadrupedal locomotion." *Neural Netw*, vol. 21, no. 4, pp. 667–681, 2008.

[14] N. Ogihara and N. Yamazaki, "Generation of human bipedal locomotion by a bio-mimetic neuro-musculo-skeletal model." *Biol Cybern*, vol. 84, no. 1, pp. 1–11, 2001.

[15] C. Paul, M. Bellotti, S. Jezernik, and A. Curt, "Development of a human neuro-musculo-skeletal model for investigation of spinal cord injury." *Biol Cybern*, vol. 93, no. 3, pp. 153–170, 2005.

[16] S. Mochon and T. McMahon, "Ballistic walking," *J. Biomech.*, vol. 13, no. 1, pp. 49–57, 1980.

[17] T. McGeer, *Principles of walking and running*, ser. Advances in Comparative and Environmental Physiology. Springer-Verlag Berlin Heielberg, 1992, vol. 11, ch. 4.

[18] R. Blickhan, "The spring-mass model for running and hopping," *J. of Biomech.*, vol. 22, pp. 1217–1227, 1989.

[19] T. McMahon and G. Cheng, "The mechanism of running: how does stiffness couple with speed?" *J. of Biomech.*, vol. 23, pp. 65–78, 1990.

[20] T. McGeer, "Passive dynamic walking," *Int. J. Rob. Res.*, vol. 9, no. 2, pp. 62–82, 1990.

[21] A. Seyfarth, H. Geyer, M. Günther, and R. Blickhan, "A movement criterion for running," *J. of Biomech.*, vol. 35, pp. 649–655, 2002.

[22] R. Ghigliazza, R. Altendorfer, P. Holmes, and D. Koditschek, "A simply stabilized running model," *SIAM J. Applied. Dynamical Systems*, vol. 2, no. 2, pp. 187–218, 2003.

[23] A. Seyfarth, H. Geyer, and H. M. Herr, "Swing-leg retraction: a simple control model for stable running," *J. Exp. Biol.*, vol. 206, pp. 2547–2555, 2003.

[24] M. Raibert, *Legged robots that balance*. MIT press, Cambridge, 1986.

[25] U. Saranli, M. Buehler, and D. Koditschek, "Rhex: A simple and highly mobile hexapod robot." *Int. Jour. Rob. Res.*, vol. 20, no. 7, pp. 616–631, 2001.

[26] S. Collins, A. Ruina, R. Tedrake, and M. Wisse, "Efficient bipedal robots based on passive-dynamic walkers," *Science*, vol. 307, no. 5712, pp. 1082–5, 2005.

[27] H. Geyer, A. Seyfarth, and R. Blickhan, "Compliant leg behaviour explains the basic dynamics of walking and running," *Proc. R. Soc. Lond. B*, vol. 273, pp. 2861–2867, 2006.

[28] A. Prochazka, D. Gillard, and D. Bennett, "Positive force feedback control of muscles," *J. of Neurophys.*, vol. 77, pp. 3226–3236, 1997.

[29] H. Geyer, A. Seyfarth, and R. Blickhan, "Positive force feedback in bouncing gaits?" *Proc. R. Soc. Lond. B*, vol. 270, pp. 2173–2183, 2003.

[30] A. Seyfarth, M. Günther, and R. Blickhan, "Stable operation of an elastic three-segmented leg," *Biol. Cybern.*, vol. 84, pp. 365–382, 2001.

[31] M. Günther, V. Keppler, A. Seyfarth, and R. Blickhan, "Human leg design: optimal axial alignment under constraints," *J. Math. Biol.*, vol. 48, pp. 623–646, 2004.

[32] H. Herr and T. McMahon, "A trotting horse model," *Int. J. Robotics Res.*, vol. 19, pp. 566–581, 2000.

[33] ——, "A galloping horse model," *Int. J. Robotics Res.*, vol. 20, pp. 26–37, 2001.

[34] H. M. Herr, G. T. Huang, and T. A. McMahon, "A model of scale effects in mammalian quadrupedal running." *J Exp Biol*, vol. 205, no. Pt 7, pp. 959–967, Apr 2002.

[35] K. Pearson and D. Collins, "Reversal of the influence of group Ib afferents from plantaris on activity in medial gastrocnemius muscle during locomotor activity," *J. of Neurophys.*, vol. 70, pp. 1009–1017, 1993.

[36] M. J. Grey, J. B. Nielsen, N. Mazzaro, and T. Sinkjaer, "Positive force feedback in human walking," *J Physiol*, vol. 581, no. 1, pp. 99–105, 2007.

[37] L. O. Christensen, J. B. Andersen, T. Sinkjaer, and J. Nielsen, "Transcranial magnetic stimulation and stretch reflexes in the tibialis anterior muscle during human walking," *J Physiol*, vol. 531, no. Pt 2, pp. 545–57, 2001.

[38] N. Petersen, H. Morita, and J. Nielsen, "Modulation of reciprocal inhibition between ankle extensors and flexors during walking in man," *J Physiol*, vol. 520 Pt 2, pp. 605–19, 1999.

[39] T. Mergner, C. Maurer, and R. J. Peterka, "A multisensory posture control model of human upright stance," *Prog Brain Res*, vol. 142, pp. 189–201, 2003.

[40] S. M. O'Connor and A. D. Kuo, "Direction dependent control of balance during walking and standing," *J Neurophysiol*, 2009.

[41] M. Günther and H. Ruder, "Synthesis of two-dimensional human walking: a test of the λ-model," *Biol. Cybern.*, vol. 89, pp. 89–106, 2003.

[42] V. T. Inman, H. J. Ralston, F. Todd, and J. C. Lieberman, *Human walking*. Baltimore: Williams & Wilkins, 1981.

[43] V. Dietz and S. J. Harkema, "Locomotor activity in spinal cord-injured persons," *J Appl Physiol*, vol. 96, no. 5, pp. 1954–60, 2004.

[44] M. Y. C. Pang and J. F. Yang, "Sensory gating for the initiation of the swing phase in different directions of human infant stepping," *J Neurosci*, vol. 22, no. 13, pp. 5734–40, 2002.

[45] C. Schneider, M. C. Do, and B. Bussel, "Increase of the contraction of the stance soleus muscle in human does not delay the swing phase in step elicited by forward fall," *C R Acad Sci III*, vol. 320, no. 9, pp. 709–14, 1997.

[46] S. N. Zill, B. R. Keller, and E. R. Duke, "Sensory signals of unloading in one leg follow stance onset in another leg: transfer of load and emergent coordination in cockroach walking," *J Neurophysiol*, vol. 101, no. 5, pp. 2297–304, 2009.

[47] T. Lam and K. G. Pearson, "Proprioceptive modulation of hip flexor activity during the swing phase of locomotion in decerebrate cats," *J Neurophysiol*, vol. 86, no. 3, pp. 1321–32, Sep 2001.

[48] J. J. Eng, D. A. Winter, and A. E. Patla, "Strategies for recovery from a trip in early and late swing during human walking," *Exp Brain Res*, vol. 102, no. 2, pp. 339–49, 1994.

[49] H. W. Van de Crommert, M. Faist, W. Berger, and J. Duysens, "Biceps femoris tendon jerk reflexes are enhanced at the end of the swing phase in humans," *Brain Res*, vol. 734, no. 1-2, pp. 341–4, 1996.

[50] J. Perry, *Gait analysis: normal and pathological function*. SLACK Inc., Thorofare, NJ, 1992.

[51] L. Li and G. E. Caldwell, "Coefficient of cross correlation and the time domain correspondence," *J Electromyogr Kinesiol*, vol. 9, no. 6, pp. 385–9, 1999.

[52] T. A. L. Wren, K. P. Do, S. A. Rethlefsen, and B. Healy, "Cross-correlation as a method for comparing dynamic electromyography signals during gait," *J Biomech*, vol. 39, no. 14, pp. 2714–8, 2006.

[53] J. U. Baumann, H. Ruetsch, and K. Schürmann, "Distal hamstring lengthening in cerebral palsy. an evaluation by gait analysis," *Int Orthop*, vol. 3, no. 4, pp. 305–9, 1980.

[54] A. J. Ijspeert, "Central pattern generators for locomotion control in animals and robots: a review." *Neural Netw*, vol. 21, no. 4, pp. 642–653, 2008.

[55] L. S. Illis, "Is there a central pattern generator in man?" *Paraplegia*, vol. 33, no. 5, pp. 239–40, 1995.

[56] A. Lundberg, "Reflex control of stepping," *In: The Nansen memorial lecture V, Oslo: Universitetsforlaget*, pp. 5–42, 1969.

[57] G. Taga, "A model of the neuro-musculo-skeletal system for human locomotion. I. Emergence of basic gait," *Biol. Cybern.*, vol. 73, no. 2, pp. 97–111, 1995.

[58] K. G. Pearson, "Generating the walking gait: role of sensory feedback." *Prog Brain Res*, vol. 143, pp. 123–129, 2004.

[59] H. Hultborn, "Spinal reflexes, mechanisms and concepts: from Eccles to Lundberg and beyond." *Prog Neurobiol*, vol. 78, no. 3-5, pp. 215–232, 2006.

[60] A. Prochazka, V. Gritsenko, and S. Yakovenko, "Sensory control of locomotion: reflexes versus higher-level control." *Adv Exp Med Biol*, vol. 508, pp. 357–367, 2002.

[61] J. M. Donelan, D. A. McVea, and K. G. Pearson, "Force regulation of ankle extensor muscle activity in freely walking cats." *J Neurophysiol*, vol. 101, no. 1, pp. 360–371, 2009.

[62] T. Sinkjaer, J. B. Andersen, M. Ladouceur, L. O. Christensen, and J. B. Nielsen, "Major role for sensory feedback in soleus EMG activity in the stance phase of walking in man." *J Physiol*, vol. 523 Pt 3, pp. 817–827, 2000.

[63] M. A. Daley, G. Felix, and A. A. Biewener, "Running stability is enhanced by a proximo-distal gradient in joint neuromechanical control." *J Exp Biol*, vol. 210, no. Pt 3, pp. 383–394, 2007.

[64] G. T. Yamaguchi, A. G.-U. Sawa, D. W. Moran, M. J. Fessler, and J. M. Winters, "A survey of human musculotendon actuator parameters," in *Multiple Muscle Systems: Biomechanics and Movement Organization*, J. Winters and S.-Y. Woo, Eds. Springer-Verlag, New York, 1990, pp. 717–778.

[65] T. Muraoka, Y. Kawakami, M. Tachi, and T. Fukunaga, "Muscle fiber and tendon length changes in the human vastus lateralis during slow pedaling," *J. Appl. Physiol.*, vol. 91, pp. 2035–2040, 2001.

[66] C. Maganaris, "Force-length characteristics of in vivo human skeletal muscle," *Acta Physiol. Scand.*, vol. 172, pp. 279–285, 2001.

[67] ——, "Force-length characteristics of the in vivo human gastrocnemius muscle," *Clin. Anat.*, vol. 16, pp. 215–223, 2003.

[68] T. Oda, H. Kanehisa, K. Chino, T. Kurihara, T. Nagayoshi, E. Kato, T. Fukunaga, and Y. Kawakami, "In vivo lenth-force relationships on muscle fiver and muscle tendon complex in the tibialis anterior muscle," *Int. J. Sport and Health Sciences*, vol. 3, pp. 245–252, 2005.

[69] S. Scott and D. Winter, "Biomechanical model of the human foot: kinematics and kinetics during the stance phase of walking," *J. Biomech.*, vol. 26, no. 9, pp. 1091–1104, 1993.